

Radiative decay lifetimes of CH_2^-

M. Okumura, L. I. Yeh, D. Normand,^{a)} J. J. H. van den Biesen,^{b)} S. W. Bustamente,^{c)} Y. T. Lee, Timothy J. Lee, Nicholas C. Handy,^{d)} and Henry F. Schaefer III
Materials and Molecular Research Division, Lawrence Berkeley Laboratory and Department of Chemistry,
University of California, Berkeley, California 94720

(Received 4 November 1986; accepted 16 December 1986)

Recently the presence and radiative decay of vibrationally excited CH_2^- , generated in a hot cathode discharge of methane, was established by measuring the time dependent photodetachment from excited states of CH_2^- as it radiatively relaxed in a high vacuum ion trap. The time dependence of the photodetachment was found to be consistent with an electron affinity of 5250 cm^{-1} (0.65 eV) for ground state \tilde{X}^3B_1 methylene. The radiative decay lifetimes of the first three excited bending vibrations of CH_2^- were also tentatively assigned. Here, we report a more refined analysis of the experimental data along with theoretical *ab initio* determinations of the radiative decay lifetimes of the first four excited bending vibrational levels of CH_2^- . There is some discrepancy between the *ab initio* values (431, 207, 118, and 68 ms for the $v_2 = 1, 2, 3$, and 4 levels respectively) and the experimental values (525, 70, and 14 ms for $v_2 = 1, 2$, and 3 respectively) for $v_2 = 2$ and 3. Possible reasons for this discrepancy are discussed but none of the alternatives are entirely satisfactory.

I. INTRODUCTION

Recently we presented¹ preliminary results for the determination of the radiative decay lifetimes of vibrationally excited CH_2^- . The main purpose of the original work was to demonstrate the existence of vibrationally excited ($v_2 \neq 0$) CH_2^- when created in a discharge. Hot bands are a potential problem in the photoelectron and photodetachment spectroscopy of negative ions created by discharge, sputter and other high temperature ion sources.^{2,3} The interpretation of the first photoelectron spectrum of the methylene anion proved to be particularly difficult⁴ because the standard techniques used to identify hot bands failed to do so. It is now well established,^{1,5,6,20} though, that hot bands were present in the photoelectron spectrum as first suggested by *ab initio* studies.⁷

Using a radio frequency (rf) ion trap at very low pressures, we were able to trap CH_2^- ions without collisions, and measure the radiative decay of the hot band signal as a function of trapping time. The decay rates of individual v_2 levels were obtained from a tentative fit of the data. In this paper we examine more carefully the radiative lifetimes of the v_2 bending vibrations of \tilde{X}^2B_1 CH_2^- . We present both *ab initio* calculations of the $v_2 = 1, 2, 3$, and 4 lifetimes and a more refined analysis of the data, including additional data not reported earlier.

Leopold *et al.*⁶ have presented photoelectron spectra of "cold" CH_2^- created in a flowing afterglow. Their work, along with a semirigid bender analysis by Sears and Bunk-

er,^{20,21} provides a clear description of this anion. The \tilde{X}^2B_1 state has a bond angle of 103° , and a barrier to linearity of approximately $10\,000\text{ cm}^{-1}$. The electron affinity^{6,21} of \tilde{X}^3B_1 CH_2 is $0.652 \pm 0.006\text{ eV}$, in excellent agreement with predictions of *ab initio* calculations. The C-H bond lengths of these two states are nearly identical, but the triplet CH_2 radical is quasilinear, with a bond angle of 134.8° , and a barrier to linearity of only 1940 cm^{-1} . As a result, the Franck-Condon overlap for $\Delta v_2 = 0$ transitions is small, and the photoelectron spectrum is characterized by a progression in the v_2 bending transition. In contrast, the low lying \tilde{a}^1A_1 state of the neutral is nearly identical in geometry to the anion, and it contributes a single large peak at $\Delta v_2 = 0$. This state lies 3165 cm^{-1} above the ground state.

Bunker and Langhoff⁸ have presented transition moment matrix elements of vibrational transitions, for \tilde{X}^3B_1 CH_2 and \tilde{a}^1A_1 CH_2 . These were determined from *ab initio* electronic structure calculations coupled with semirigid bender (SRB) vibrational wave functions. In fact we used¹ the \tilde{a}^1A_1 CH_2 data in the comparison of the radiative decay lifetimes of \tilde{X}^2B_1 CH_2^- and \tilde{a}^1A_1 CH_2 . Although these states have similar geometries and bending potentials, their dipole moments differ considerably and so may the dipole moment surfaces. A comparison of the neutral and anion lifetimes can be of only limited usefulness.

Because the CH_2^- bending vibration is a large amplitude motion, a large part of the potential and dipole moment surfaces are sampled. Such calculations are relatively difficult, and have not been systematically investigated.

It is a well-known fact that highly accurate *ab initio* predictions for anions are difficult, requiring extremely large basis sets coupled with highly correlated wave functions. In a recent study Lee and Schaefer⁹ demonstrated that even at the self-consistent-field (SCF) level of theory rather large basis sets are necessary in order to "converge" many molecular properties. Thus, it was necessary first to determine the size and type (i.e., how many *s*, *p*, and *d* functions) of basis

^{a)} Permanent address: C. E. N./Saclay, Dph. G/S. P. A. S., 91191, Gif-sur-Yvette, France.

^{b)} Permanent address: WAS 1414 Philips Research Laboratories, Postbox 8000, 5600 J. A. Eindhoven, Netherlands.

^{c)} Permanent address: Hughes Aircraft Corp., P. O. Box 2999, Torrance, CA 90509.

^{d)} Permanent address: University Chemical Laboratory, Lensfield Road, Cambridge, CB2 1EW, England.

set needed at the configuration interaction (CI) level of theory. Though it is not the purpose of this paper to detail the results of the basis set study as that will be done in a later publication,¹⁰ an indication of the sensitivity to the basis of several geometrical properties will be given.

Of course many studies of polyatomic anionic species have involved the use of correlated wave functions, but to the best of our knowledge, none have explicitly investigated the basis set dependence on all the properties of interest here, namely geometrical structure, surface shape and most importantly, the shape of the dipole moment surface. It is noteworthy that Werner, Rosmus, and co-workers^{11–13} have theoretically investigated OH^- , C_2^- , NH^- , and CH^- and Botschwina^{14–16} has studied CN^- , CCH^- , and NH_2^- . Werner, Rosmus, and Reinsch¹¹ demonstrated the need of a multiconfiguration self-consistent-field (MCSCF) reference wave function for diatomics, but this undoubtedly is due in large part to the inadequate description of the dissociation process which plague many restricted Hartree–Fock (RHF) SCF wave functions. We believe that for the type of molecular motion which is being studied here, specifically the bending mode in a symmetric, nonlinear triatomic, the SCF wave function should give a good zeroth order description. The one possible exception to this may be when the HCH angle is very small (i.e., $\text{CH}_2^- \rightarrow \text{C}^- + \text{H}_2$). However, we did not see any evidence for the deterioration of the single configuration reference function as the bond angle decreased. Further support for this argument can be found in a recent study on the effects of triple and quadruple excitations on the harmonic vibrational frequencies of several molecules,¹⁷ where it was found that these higher excitations contributed very little to bending harmonic frequencies.

In Botschwina's study¹⁴ of NH_2^- he did not include the dipole moment or the infrared (IR) intensities. Also, though the final basis is rather large,^{11–16} only one basis set is used for CCH^- and NH_2^- and two for CN^- . Thus it is difficult to deduce any basis set dependencies.

It is also of interest to note the recent work of Adler-Golden, Langhoff, Bauschlicher, and Carney (ALBC) on the ozone molecule.¹⁸ Although O_3 is not an anion, ALBC's work is relevant because of their success in reproducing the experimental IR intensities, which depend upon the same transition moment matrix elements as do vibrational radiative decay lifetimes. Using a complete active space self-consistent-field (CASSCF) wave function to compute the dipole moment function and an experimental potential function, ALBC obtain IR intensities in reasonable quantitative agreement with experiment for fundamentals, hot bands and combination bands. ALBC computed the energy and dipole moment for more than 200 points of the CASSCF Born–Oppenheimer potential energy surface and then used a variational approach to solve for the vibrational wave functions.

The goal of the present study is to determine the radiative decay lifetimes of the bending mode in CH_2^- with qualitative and semiquantitative accuracy. Since it is believed that the ν_2 fundamental and combinations thereof are reasonably far removed from the ν_1 and ν_3 fundamentals (and combinations) it is a reasonable approximation to ignore their cou-

pling. Therefore, the SRB model Hamiltonian¹⁹ of Bunker and Landsberg is a useful method for obtaining the bending vibrational wave functions. Equally important is the existence of an empirically derived SRB potential function^{20,21} for CH_2^- . This will enable the purely *ab initio* radiative decay lifetimes to be compared with those obtained with the empirical potential and the *ab initio* dipole moment function.

The reader should realize that CH_2^- is a Renner–Teller molecule like the carefully studied NH_2 molecule. The barrier to linearity is on the order of $10\,000\text{ cm}^{-1}$, and in this paper we are only considering vibrational levels up to approximately 5000 cm^{-1} above the lower state (2B_1) minimum. Furthermore we are also only considering $J=0$ states. Experimental evidence cannot distinguish between rotational effects and the results presented here represent a Boltzman average of these effects. With these restrictions the theoretical analysis is considerably simplified because if $J \neq 0$, a correct theory must involve both the 2B_1 and 2A_1 surfaces. However, if the similarity between CH_2^- and NH_2 is realized then one would expect the Renner–Teller couplings to be small for small ν quantum numbers and $J \neq 0$.

The details of the experiment and the analysis of the data are presented in Sec. II. In Sec. III the *ab initio* methods and results are presented. Finally, in Sec. IV we discuss and relate the theoretical and experimental results from the two previous sections.

II. EXPERIMENT

A. Experimental details

Radiative decay rates of vibrationally excited ions can be measured, free of collisions, using the ion trapping technique. This technique is especially suitable for excited states with lifetimes longer than 1 ms, which are difficult to measure by more conventional techniques. A problem with ion trapping experiments lies in the low densities of ions that can be trapped, making it difficult to directly observe emitted photons. Instead, many such measurements probe the excited state population as a function of trapping time by other means. For negative ions, one can measure the photodetachment signal using photons with energies less than the electron binding energy for the ground state and greater than that for the excited states. Electrons will be detached only from ions in excited states. At a given trapping time, the depletion caused by a laser pulse will provide a measure of the population of all those excited states which are bound by energies less than the photon energy. The relative signal from each state will depend upon the cross section for photodetachment.

The experimental apparatus, shown schematically in Fig. 1, is described in detail elsewhere.^{22,23} The machine is a tandem mass spectrometer, with a radio frequency (rf) octopole ion trap. A magnet mass filter first mass selects a beam of CH_2^- ions. These ions are then injected into the octopole ion trap, where they are stored for some trapping time. The population of excited state ions is then probed with a pulsed laser tuned to a desired photon frequency. The remaining ions are released, mass analyzed, and counted. An identical cycle is repeated, with the laser off. The relative difference between the two cycles gives the average laser-induced de-

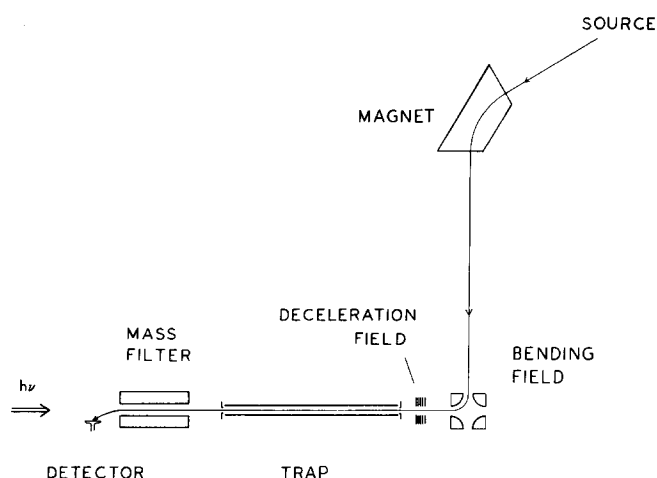


FIG. 1. Schematic of ion spectrometer.

pletion at that trapping time. We obtain the radiative decay by incrementing the trapping time and measuring the remaining excited state populations.

The methylene anions were created in a duoplasmatron source, in a discharge of 30 to 300 mTorr of 99.999% pure methane (Matheson ultrahigh purity), with typical discharge currents of 1–2 mA. Like the Branscomb source used in the early photoelectron experiments on CH_2^- , this source was a hot cathode discharge. To help confine the plasma, an external magnetic field was applied and an intermediate electrode was placed between the anode and cathode. A tungsten rod ran down the center of the source, as previous work has shown that this aided in negative ion formation. The ions were extracted from the source, accelerated to approximately 350 eV, and mass-selected with a 20 cm radius sector magnet. An electrostatic quadrupole field deflected the ion beam 90° . The ions were then focused and decelerated to approximately 0.5 eV upon entering the trap.

We trapped the ions inside a 50 cm long rf octopole ion guide. The octopole was constructed of eight 50 cm long rods, 0.3 cm in diameter, symmetrically placed on a circle of 1.25 cm diam. By applying opposite phases of rf to alternate rods, an oscillating octopole field was created, which effectively trapped the ion motion transverse to the axis of the trap. The ions were confined inside the octopole by the dc potentials of lens elements on either end of the octopole. The pressure in the trap region was approximately 3×10^{-9} Torr.

For 0.5 to 1 ms, the lens element at the entrance of the trap was kept at a potential to focus the ions into the trap. The lens potential was then raised to 10 eV above the dc bias of the trap, confining the ions in the trap and stopping further ions from entering. After a delay interval, during which excited ions would decay, the laser was fired into the trap. The ions were then released from the trap, mass analyzed, and detected with a ceratron electron multiplier. The data cycle was repeated, with the laser off. After averaging many pairs of cycles, the difference gave the average depletion at that trapping time. Decay curves were generated by incrementing the trapping time and measuring the fractional depletion.

We used a simple optical parametric oscillator (OPO) as our source for tunable infrared radiation. The OPO was a LiNbO_3 crystal in a simple cavity with no grating, pumped by the far field of a Quanta Ray Nd:YAG laser. We operated the laser at degeneracy (4700 cm^{-1}), where the linewidth of 200 cm^{-1} and pulse energy of 10 to 18 mJ were anomalously large. The laser repetition rate was kept at a constant 10 Hz. For scans with delays greater than 40 ms, the OPO pulse was selected with a shutter.

B. Results

The decay of the photodetachment signal at 4700 cm^{-1} is shown in Fig. 2. Since our preliminary report,¹ we have obtained additional data recorded at the short times. The decay is clearly not a single exponential. In contrast, at a photon energy of 9394 cm^{-1} , approximately 67% of the ions are photodetached at all trapping times. The power dependence, shown in Fig. 3, reveals at least three different components, two of which are saturated. After 30 ms, the state with the largest cross section has disappeared.

The photon energy of 4700 cm^{-1} is 500 cm^{-1} (0.06 eV) less than the electron binding energy. The multiple exponential decay arises because all states with more than 500 cm^{-1}

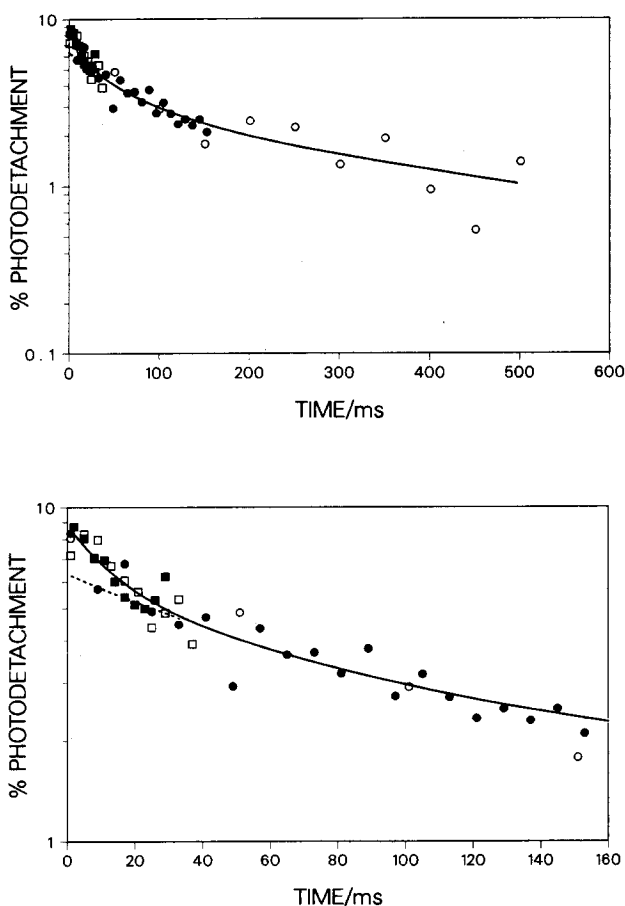


FIG. 2. Decay of the photodetachment signal at 4700 cm^{-1} . Curve is best fit of a triple exponential to the data, with lifetimes of 525, 70, and 14 ms. Lower plot shows detail of the first 160 ms of the upper plot. The solid line is from a nonlinear least-squares fit to a sum of three exponentials. The dashed line is from a fit to a sum of four exponentials, using the theoretical lifetimes for $v_2 = 1$ through 4.

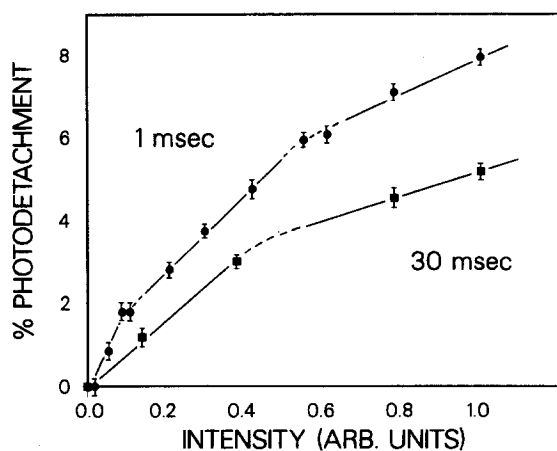


FIG. 3. Power dependence of the photodetachment signal at 4700 cm^{-1} , taken at two trapping times (a) 1 ms and (b) 30 ms.

of internal energy can be photodetached. Assuming a temperature of 2500 K, derived from the photoelectron spectra by Sears and Bunker, the relative v_2 populations are 53%, 25%, 12%, 6%, and 3% for $v_2 = 0$ through 4. The contribution to the photodetachment signal from each v_2 state depends upon the Franck–Condon factors as well as the number of final v_2 states accessible. The large change in the equilibrium bond angle and the bending potential causes the oscillator strength to be spread over several Δv_2 bands. The higher v_2 levels have more detachment channels available, and thus have larger cross sections at this photon energy.

The problem of cascading decays of an N -level system is an elementary problem of formal kinetics, for which the set of first order differential equations can be solved analytically. The solution requires initial populations, all decay rates A_{ij} (i.e., the Einstein coefficients for the transition from state i to j), and, for our data, relative photodetachment cross sections σ_i . A unique fit of our data with such a large number of parameters is impossible, but the solution can be reduced to a simple sum of exponentials

$$Y(t) = \sum_{i=1}^N Y_i e^{-t/\tau_i}, \quad (1)$$

where τ_i is the radiative decay lifetime of the i th level, and the effective preexponential factor Y_i is a function of the initial populations, the A_{ij} 's, and the photodetachment cross sections. The data were fit to Eq. (1) using the τ_i 's and the Y_i 's as parameters.

The data were fit by a weighted nonlinear least squares to the sum of exponentials. Such a fit is notoriously difficult, especially if the decay rates are similar. We fit the data to a sum of three exponentials, and obtained lifetimes of 14 ± 7 , 70 ± 50 , and 500 ± 300 ms as reported (with the preexponential factors) in Table I. In general, the most reliable fits require data over a time span covering two lifetimes. The large uncertainty in the longest lifetime stems from the lack of data beyond 500 ms. A biexponential decay mechanism, yielding lifetimes of 20 and 296 ms, gave a significantly poorer fit. The signal-to-noise was too poor to yield a unique fit to a four-exponential model.

TABLE I. Experimental lifetimes derived from fits of the data with sums of exponentials.

v_2	Three exponentials		Four exponentials ^a	
	Y_i	τ_i	Y_i	τ_i
1	2.6%	500 ms	3.1%	405 ms
2	3.2%	70	0.6%	135
3	3.0%	14	2.3%	45
4			2.8%	15

^a τ_i were constrained to a geometric progression, with ratio $\tau_i/\tau_{i+1} = 3.0$.

III. THEORY

A. Theoretical approach

All of the basis sets employed in this study embody the same starting point which is a $[7s4p/3s]$ contraction of the $(12s7p/6s)$ primitive sets of van Duijneveldt²⁴ for C and H, respectively. The contraction scheme used allows maximum flexibility in the valence region. A set of diffuse s and p functions [$\alpha_s(\text{C}) = 0.039\,906$, $\alpha_p(\text{C}) = 0.030\,237$] was added to the C sp basis and one set of diffuse s functions was added to the H basis [$\alpha_s(\text{H}) = 0.030\,155$]. The smallest basis investigated contained two sets of polarization functions [$\alpha_d(\text{C}) = 1.5$ and 0.35 ; $\alpha_p(\text{H}) = 1.4$ and 0.25] on both C and H. This basis is designated $[8s5p2d/4s2p]$ and is labeled TZ + diffuse + 2P as it was previously.⁹ The contraction coefficients are also listed in Ref. 9. The second basis investigated had another set of diffuse sp functions added [$\alpha_s(\text{C}) = 0.015\,545$; $\alpha_p(\text{C}) = 0.011\,808$; $\alpha_s(\text{H}) = 0.010\,310$] and is labeled TZ + 2 diffuse + 2P. The third basis set can be designated TZ + diffuse + 3P' where now there are three sets of polarization functions on C [$\alpha_d(\text{C}) = 2.25, 0.75, 0.25$]. Later it was found preferable to incorporate a set of more diffuse polarization functions into the C basis and so the TZ + diffuse + 3P basis consists of $\alpha_d(\text{C}) = 0.75, 0.25, 0.083$ for the carbon d functions. The final two bases were arrived at by adding yet another set of polarization functions to the carbon atomic basis. The basis labeled TZ + diffuse + 4P' has an additional C d function with an exponent $\alpha_d = 2.25$ whereas the basis labeled TZ + diffuse + 4P has a more diffuse polarization function, $\alpha_d = 0.028$. The CI's included all configurations resulting from single and double replacements from the SCF reference wave function and hence are classified CISD. All CISD calculations were carried out with the shape-driven graphical unitary group approach CI method²⁵ and geometry optimizations used analytic CI gradient techniques.^{26,27} The CI dipole moment was evaluated with respect to the center of mass as an energy derivative.^{28,29} It is worthy of noting that we support the authors of Refs. 28 and 29 in their view that the dipole moment should be calculated as an energy derivative rather than an expectation value; the reason being that the extra term which occurs (the non-Hellmann–Feynmann term) can be argued to be the correction of the CI wave function towards its MCSCF wave function.²⁷

To give an idea of the basis set dependence Table II contains the CISD equilibrium geometry, and Table III

TABLE II. CISD equilibrium geometries of CH₂⁻ using several basis sets. Bond lengths in Å and bond angles in degrees. See the text for description of basis sets.

Basis set	<i>r</i> _{C-H}	∠HCH
TZ + diffuse + 2P	1.116	102.5
TZ + 2 diffuse + 2P	1.116	102.5
TZ + diffuse + 3P'	1.116	102.6
TZ + diffuse + 3P	1.122	102.5

gives the CISD dipole moment of CH₂⁻ for several basis sets. The results depicted in Tables II and III demonstrate the need of very diffuse polarization functions for anions at the CISD level of theory. This is especially true for the dipole moment where the TZ + diffuse + 3P' value (1.97 D) is reduced to 1.72 D with the TZ + diffuse + 3P basis set. Since the TZ + diffuse + 4P dipole moment is only 0.03 D less than the TZ + diffuse + 3P value, the dipole moment function was determined initially with the TZ + diffuse + 3P basis, and later with the TZ + diffuse + 4P basis set.

In the SRB model¹⁹ the effective bending potential and the bond length as a function of the supplement to the bond angle are required. The supplement is defined as $\rho = \pi - \alpha$ where α is the bond angle. The dipole moment function must also be a function of ρ . Therefore, the procedure we used was to optimize the C-H bond length (i.e., until $\partial E_{\text{CI}}/\partial r_{\text{C-H}} \cong 0$) at specific bond angles. The potential, bond length, and dipole moment were then fit to a Taylor series expansion about linearity (at linearity $\rho = 0$). Because of the symmetry about linearity, only even powers of ρ appear in the potential and bond length functions and only odd powers of ρ appear in the dipole moment function. These functions (derived from the TZ + diffuse + 3P basis) are given in Eqs. (2) through (4) with the units being cm⁻¹, Å, and D, respectively.

$$V(\rho) = -13\,951\rho^2 + 6733.1\rho^4 - 1555.7\rho^6 + 238.95\rho^8 - 16.101\rho^{10}, \quad (2)$$

$$r_{\text{C-H}}(\rho) = 1.081\,844 + 0.023\,014\,0\rho^2 - 0.000\,506\rho^4, \quad (3)$$

$$\mu(\rho) = 3.033\,421\rho - 1.914\,737\rho^3 + 0.893\,442\rho^5 - 0.295\,384\rho^7 + 0.062\,339\rho^9 - 0.007\,390\rho^{11} + 0.000\,372\rho^{13}. \quad (4)$$

The potential and dipole moment functions were least-

TABLE III. CISD total energies (hartrees) and dipole moments (debyes) of CH₂⁻ using several basis sets. Each dipole moment was evaluated as an energy derivative. See the text for details concerning the basis sets.

Basis set	Geometry of calculation	<i>E</i> _{CISD}	μ
TZ + diffuse + 2P	Same method	-39.088 974	1.98
TZ + 2 diffuse + 2P	Same method	-39.089 076	2.00
TZ + diffuse + 3P'	Same method	-39.092 463	1.97
TZ + diffuse + 3P	Same method	-39.089 542	1.72
TZ + diffuse + 4P	TZ + diffuse + 3P	-39.089 639	1.69
TZ + diffuse + 4P'	TZ + diffuse + 3P	-39.093 362	1.76

squares fit from 18 points with α , the bond angle, ranging from 60° to 148°. The bond length function used only 13 points even though the bond was optimized for each angle α . Only 13 points were used here in order to minimize the variance of the fit. However, the bending energy levels as well as the transition moment matrix elements were quite insensitive to the bond length function used as long as it had the form of Eq. (3). These functions are shown in Figs. 4–6. Also depicted in Figs. 4 and 5 are the potential and dipole moment functions obtained with the TZ + diffuse + 4P basis. These calculations were performed at the TZ + diffuse + 3P geometries. The explicit forms of the functions are

$$V(\rho) = -14\,042\rho^2 + 6870.5\rho^4 - 1637.08\rho^6 + 259.97\rho^8 - 18.050\rho^{10}, \quad (5)$$

$$\mu(\rho) = 3.336\,752\rho - 2.715\,518\rho^3 + 1.748\,393\rho^5 - 0.793\,873\rho^7 + 0.225\,337\rho^9 - 0.035\,182\rho^{11} + 0.002\,281\,6\rho^{13}. \quad (6)$$

We did not consider asymmetric geometries for the following reasons. As noted previously, Bunker and Langhoff⁸ have reported transition moment matrix elements for \tilde{a}^1A_1 CH₂ using an empirically derived SRB potential with an *ab initio* dipole moment function. These were used by us previously⁸ to determine the radiative decay lifetimes of the $v_2 = 1, 2$, and 3 states. Their dipole moment function has the form⁸

$$\mu_b = p \sin(c\rho) + q \sin^2(c\rho) + \mu'_b S_1 \quad (7)$$

and

$$\mu_a = \mu'_a S_3, \quad (8)$$

where $S_1 = (\Delta r_1 + \Delta r_2)/2^{1/2}$, $S_3 = (\Delta r_1 - \Delta r_2)/2^{1/2}$, $\rho = \alpha - \pi$, and $\Delta r_i = r_i - r_e$. Equation (8) deals with asymmetric geometries and as noted we did not consider these. The last term in Eq. (7) allows for the change in the dipole moment with respect to changes in the bond length, and hence has more flexibility than our functional form. However, if this term is neglected the radiative decay lifetimes of \tilde{a}^1A_1 CH₂ change by only +3, +1, and -4 ms for the $v_2 = 1, 2$, and 3 levels, respectively. Thus we were not

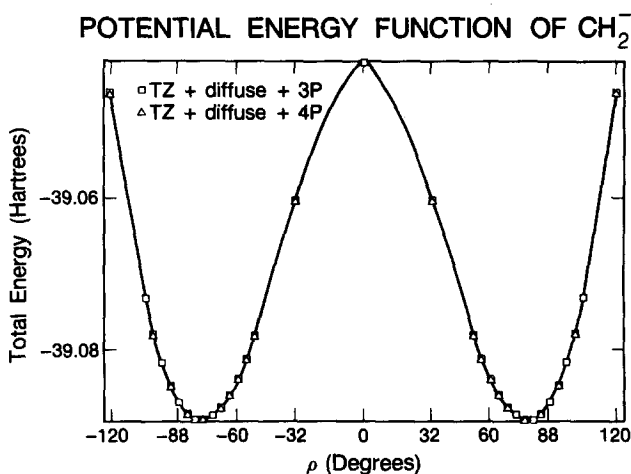


FIG. 4. *Ab initio* potential energy curves for CH₂⁻. See the text for details of the basis sets.

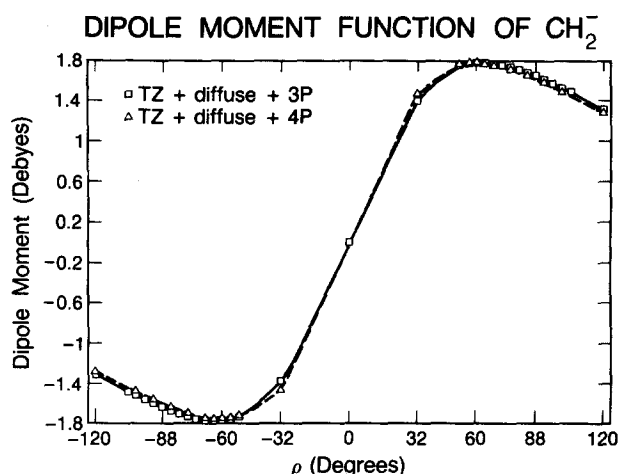


FIG. 5. *Ab initio* dipole moment curves for the bending mode of CH_2^- . See the text for details.

compelled to incorporate a like term into the CH_2^- dipole moment function.

We also found it difficult to use the functional form of Eq. (7). We found it much easier to use a Taylor series expansion due to the shape of the dipole curve for CH_2^- . Figure 5 has a plot of the CISD dipole curves obtained from the TZ + diffuse + 3P basis and TZ + diffuse + 4P basis sets.

B. Radiative decay lifetimes

The determination of a radiative decay lifetime is rather straightforward and has been briefly reviewed by McKellar⁵ and co-workers. The radiative decay lifetime of the $v_2 = i$ vibrational state is given by

$$\tau_i = 1 / \sum_j A_{ij}, \quad (9)$$

where the Einstein A_{ij} coefficient is given by

$$A_{ij}/\text{s}^{-1} = \frac{64\pi^4}{3hc^3} (\omega_{ij}/\text{cm}^{-1})^3 |\langle i|\mu/D|j\rangle|^2 \quad (10)$$

$$= 3.14 \times 10^{-7} (\omega_{ij}/\text{cm}^{-1})^3 |\langle i|\mu/D|j\rangle|^2. \quad (11)$$

Here ω_{ij} is the difference of the vibrational levels $|i\rangle$ and $|j\rangle$,

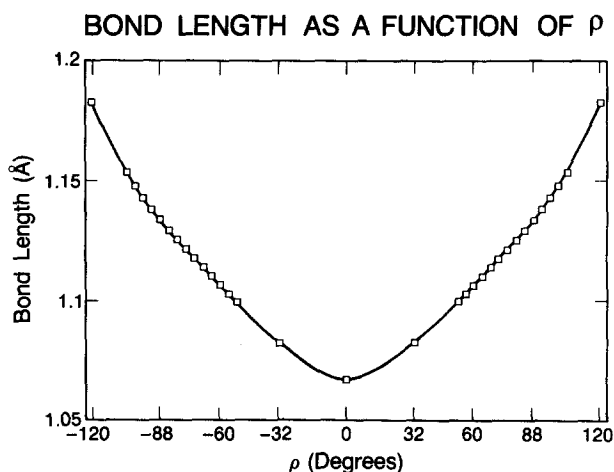


FIG. 6. The *ab initio* optimum bond length of CH_2^- for various HCH angles. The TZ + diffuse + 3P basis was used. See the text for details of this basis.

TABLE IV. Radiative decay lifetimes (ms) of the bending vibrational states of CH_2^- . The first column represents a purely *ab initio* value whereas the remaining columns coupled empirical potentials with an *ab initio* dipole moment function.^a

v_2	<i>Ab initio</i> ^b	Empirical ^c	Empirical ^d
1	431 (574)	471 (615)	491 (661)
2	207 (232)	231 (258)	231 (257)
3	118 (114)	134 (135)	129 (125)
4	68 (60)	82 (76)	75 (67)

^a Values in parentheses were obtained with the TZ + diffuse + 3P basis while the others incorporated the TZ + diffuse + 4P basis.

^b Purely *ab initio* values obtained with the appropriate basis. See the text for details.

^c See Ref. 20 for the first empirically derived SRB potential.

^d See Ref. 21 for the second empirically derived SRB potential.

where $|j\rangle$ are the vibrational levels below $|i\rangle$. In the model used here the $|i\rangle$ and $|j\rangle$ are the SRB wave functions.

Table IV contains the purely *ab initio* radiative decay lifetimes along with those obtained with the two SRB potentials of Sears and Bunker^{20,21} coupled with the *ab initio* dipole moment function. As can be seen, there are not large differences between the sets of values. The results of Table IV indicate that the *ab initio* potential function is quite adequate and that the radiative decay lifetimes are very sensitive to the dipole moment function. Further support for the high quality of the *ab initio* potential is presented in Table V where the SRB vibrational energy levels for the various potential functions are given. The theoretical potentials agree with the empirically derived potentials reasonably well, especially in the lower levels.

The transition moment matrix elements and Einstein A coefficients used in determining the radiative decay lifetimes are listed in Tables VI and VII, respectively. As is expected, the absolute value of the transition moment matrix elements is largest for adjacent vibrational levels.

Not quite so easily predicted is the relationship of the Einstein A coefficients with Δv_2 . For the $i = 3, 4$ levels the Einstein A_{ij} coefficient is largest for $\Delta v_2 = 2$. Also interesting to note is that although the radiative decay lifetimes derived from the empirical potentials are very similar, the individual Einstein A coefficients are somewhat different and in fact the most recent potential²⁵ agrees much better with the *ab initio* results.

TABLE V. Bending vibrational energy levels determined from the semirigid bender (SRB) wave functions. Units are cm^{-1} .

v_2	<i>Ab initio</i> ^a		Sears and Bunker ^b	Bunker and Sears ^c
	TZ + diffuse + 3P	TZ + diffuse + 4P	Bunker ^b	Sears ^c
0	638	638	591	604
1	1934	1933	1789	1835
2	3212	3210	2970	3043
3	4466	4465	4131	4227
4	5689	5689	5272	5382

^a This work.

^b Reference 20.

^c Reference 21.

TABLE VI. Transition moment matrix elements between the bending vibrational levels. Semirigid bender (SRB) vibrational wave functions were coupled with the TZ + diffuse + 4P dipole moment function.^a The SRB wave functions were determined from both *ab initio* and empirically derived potential energy functions.

v_2	v_2'	<i>Ab initio</i>	Empirical ^b	Empirical ^c
1	0	0.058 35 (0.050 50)	0.062 77 (0.054 93)	0.059 08 (0.050 90)
2	0	-0.015 99 (-0.018 90)	-0.014 14 (-0.017 58)	-0.016 70 (-0.019 81)
2	1	0.072 71 (0.060 57)	0.082 26 (0.070 51)	0.074 36 (0.061 70)
3	0	-0.003 28 (-0.003 35)	-0.005 04 (-0.005 54)	-0.003 58 (-0.003 67)
3	1	-0.030 63 (-0.035 69)	-0.026 60 (-0.032 05)	-0.031 81 (-0.037 11)
3	2	0.075 61 (0.058 39)	0.093 01 (0.076 34)	0.078 54 (0.060 57)
4	0	-0.000 07 (-0.000 01)	-0.000 95 (-0.000 68)	-0.000 11 (0.000 01)
4	1	-0.006 14 (-0.006 74)	-0.009 50 (-0.011 35)	-0.006 66 (-0.007 40)
4	2	-0.048 73 (-0.055 31)	-0.041 47 (-0.048 01)	-0.050 34 (-0.057 05)
4	3	0.068 57 (0.045 43)	0.097 16 (0.075 04)	0.073 17 (0.049 12)

^a Values in parentheses are due to the TZ + diffuse + 3P basis.

^b See Ref. 20.

^c See Ref. 21.

One way of testing the qualitative reliability of the theoretical decay lifetimes would be to determine the τ_1 lifetimes incorporating the double harmonic approximation (i.e., using mechanical and electrical harmonicity which means truncating the potential at quadratic terms and the dipole moment function at linear terms). Harmonic vibrational frequency and IR intensity determinations for small molecules are becoming quite common, even at the CISD level of theory. Using the TZ + diffuse + 3D basis we obtain $\omega_1 = 2782$, $\omega_2 = 1314$, and $\omega_3 = 2841$ cm⁻¹ with the corresponding IR intensities being 633, 12, and 363 km/mol, respectively. Using the *ab initio* dipole derivatives we determine the radiative decay lifetime of the first excited vibrational state to be $\tau_1 = 1.6, 385$, and 2.7 ms for the ν_1, ν_2 , and ν_3 modes, respectively. The ν_2 value is qualitatively similar to the value obtained with the SRB bending wave functions with this basis, 574 ms.

IV. DISCUSSION

There are few calculations of vibrational intensities or lifetimes for polyatomic ions whose accuracy can be verified by experiment. Theoretical values of the $\nu = 1$ lifetime of

CH⁻ agree to within 10% of the experimental value obtained in our laboratory, but the strong CH bond means that CH⁻ can be approximated by a harmonic oscillator quite reliably. A method such as the semirigid bender model used here should be more accurate than using the harmonic oscillator approximation.

The results of the current fit to three exponentials are similar to the previous experimental results.¹ We have initially assigned the three observed decays of 500, 70, and 14 ms to $\nu_2 = 1, 2$, and 3 , respectively. The longest lifetime, 500 ms, agrees reasonably well with our theoretical $\nu_2 = 1$ lifetime of 431 ms. The latter is the most reliable of the theoretical lifetimes. The experimental values for the $\nu_2 = 2$, and $\nu_2 = 3$ (70 and 14 ms), however, are significantly smaller than the theoretical values of 207 and 108 ms. Thus, the lifetimes obtained from a fit with a three-exponential model do not agree with theory.

The five- to sevenfold decrease in the experimental lifetimes with vibrational quantum number, however, seems anomalously large. The theoretical lifetimes decrease by only a factor of about 2 for each additional quantum in the bending mode. It is quite possible that an additional component with an intermediate lifetime is present but cannot be

TABLE VII. Einstein *A* coefficients for the coupling of bending vibrational levels. The semirigid bender (SRB) bending vibrational wave functions were coupled with the TZ + diffuse + 4P dipole moment function.^a Both *ab initio* and empirical potential functions were used. Units are s⁻¹.

v_2	v_2'	<i>Ab initio</i>	Empirical ^b	Empirical ^c
1	0	2.319 69 (1.741 33)	2.123 96 (1.626 50)	2.037 09 (1.512 03)
2	0	1.364 63 (1.910 45)	0.843 36 (1.304 59)	1.268 54 (1.785 34)
2	1	3.457 04 (2.399 81)	3.491 27 (2.564 80)	3.060 30 (2.107 21)
3	0	0.189 50 (0.197 07)	0.353 79 (0.427 03)	0.190 78 (0.200 53)
3	1	4.775 57 (6.480 85)	2.850 97 (4.139 62)	4.344 64 (5.914 91)
3	2	3.538 32 (2.107 50)	4.252 78 (2.864 84)	3.209 85 (1.909 33)
4	0	0.000 22 (0.000 00)	0.029 24 (0.014 93)	0.000 42 (0.000 00)
4	1	0.627 10 (0.754 23)	1.195 63 (1.707 73)	0.620 06 (0.766 94)
4	2	11.340 29 (14.590 12)	6.584 13 (8.825 56)	10.172 50 (13.065 43)
4	3	2.705 66 (1.185 53)	4.397 18 (2.623 02)	2.588 48 (1.166 45)

^a Values in parentheses are due to the TZ + diffuse + 3P basis.

^b See Ref. 20 for the empirically derived SRB potential.

^c See Ref. 21 for the empirically derived SRB potential.

extracted from the data due to the signal-to-noise. Examination of the data reveals that there are not enough data points between 150 and 300 ms to preclude the existence of such a component.

The discrepancy between the results of the fit and theory indicate that four exponentials may be necessary. Although an unconstrained fit (eight parameters) of the data to a sum of four exponentials does not yield a unique result, we can fit the data if we reduce the number of variables. The trend in the theoretical results suggest that we can assume a geometric progression for the four lifetimes. Therefore, we have performed several fits holding the ratio τ_i/τ_{i+1} constant. The range of lifetimes is large, and the lowest value of τ_i/τ_{i+1} that fits the data is 3.0, with lifetimes of 15, 45, 135, and 405 ms. The $v_2 = 1$ lifetime agrees with the *ab initio* value, and the $v_2 = 2$ lifetime is somewhat closer to the theoretical result, but the two smaller lifetimes are still significantly less than theory. Therefore, the lifetimes extracted from the data using a four-component model with constant τ_i/τ_{i+1} still do not completely agree with the theoretical results. Furthermore, the ratio $\tau_i/\tau_{i+1} = 2.5$ gives a fit one standard error worse than the best fit, with lifetimes of 19, 47, 118, and 296 ms. Thus we cannot fit the data with the theoretical τ_i/τ_{i+1} of approximately two for a geometric progression of four lifetimes.

We have also tried to fit the experimentally observed curve in Fig. 1, setting all the τ_i to the theoretical values, but have found that the data cannot be fit. The dashed curve in Fig. 2 is the result of such an attempt. Despite the ambiguities in fitting a multiple exponential decay, it is clear that the theoretical values for $v_2 = 1$ through 4 cannot reproduce the experimentally observed decay. The problem lies at the shortest times ($\tau < 30$ ms), where the experimental signal-to-noise is best, and the theory is the most uncertain.

The deviation of the dashed curve from the data suggest an alternative explanation for the disagreement. If the theoretical values for τ_i for $i = 1, 2$, and 3 are used, along with a fourth decay that is allowed to vary, the data can be fit, with $\tau_4 = 15$ ms. This result implies that the theoretical results would be consistent with experiment if one postulates an alternative relaxation mechanism giving rise to a fast decay. We next consider possible sources for a fast decaying component.

The fast decay component could be the result of an experimental artifact; however, we have made a similar measurement of the excited state lifetimes of CH^- under almost identical experimental conditions, and observed lifetimes of 1.75 ms and 5.9 s,²³ but no evidence for a decay of 14 ms. For that system, we also found that collision-induced decay rates were much less than 1 s^{-1} . At the pressure used in this experiment, it is unlikely that collisions would be responsible for a process with a lifetime as fast as 14 ms. Furthermore, contamination from other species is probably not a problem. The mass resolution of the sector magnet is high: $M/\Delta M \approx 150$. The only contaminants would be isotopes of CH^- , but the lifetimes we observed for CH^- would not account for a 14 ms decay. We therefore believe that the 14 ms lifetime arises from the decay of an excited rovibrational state of $^2B_1 \text{CH}_2^-$.

If we extend the *ab initio* results to include the $v_2 = 5$

state a lifetime of 40 ms is obtained with the TZ + diffuse + 4P data. This value is somewhat longer than the observed lifetime. In addition, two objections might be raised to this possible explanation of the 15 ms experimental lifetime. First, even at a vibrational temperature of 2500 K, only 1.5% of the total population is expected to be in this level. Second, $v_2 = 5$ lies well above the threshold for electron detachment, and is therefore only metastable to electron loss.

We have thus far neglected contributions from the excited stretches $v_1 = 1$ and $v_3 = 1$. Based on isotope shifts and the Teller–Redlich rule, Leopold *et al.* estimate that the CH_2^- vibrational frequencies for v_1 and v_3 are 2580 and 2635 cm^{-1} , respectively. The theoretical harmonic values reported here (2782 and 2841 cm^{-1} , respectively) are in reasonable agreement with these estimates, with both theoretical values being 7.8% higher. Bunker and Langhoff⁸ have calculated the stretching transition moments for the neutral $\tilde{a}^1A_1 \text{CH}_2$, in the double harmonic approximation. These yield radiative lifetimes of approximately 15 and 28 ms for v_1 and v_3 , respectively. These lifetimes match the fast component we observed. However, performing the analogous calculation of CH_2^- (using the TZ + diffuse + 3P basis results) yields lifetimes of 1.6 and 2.7 ms, respectively, for the v_1 and v_3 modes. Also, these excited states are expected to have very small relative cross sections for photodetachment. The small change in the CH bond length (1.116 Å for $^2B_1 \text{CH}_2^-$ and 1.08 Å for $^3B_1 \text{CH}_2$) results in very poor Franck–Condon factors for transitions of the stretches with $\Delta v \neq 0$. No such transitions have been reported in any of the photoelectron spectra published to date. We observed that the fast component possessed a large relative cross section, with the transition seemingly saturated at the intensities used in our experiment. Thus, it is difficult to reconcile the observed cross section with the expected poor Franck–Condon overlap, and the estimated lifetimes of the stretches are not entirely consistent either.

In our calculation, we did not consider the possibility of a Fermi resonance. Because the stretching modes have relatively large transition moments, the strong coupling of a stretching mode with a bending level $v_2 = n$ could greatly reduce the lifetime of the latter. The $v_2 = 1$ frequency of 2580 cm^{-1} estimated by Leopold *et al.* is very close to the $v_2 = 2$ level at 2572 cm^{-1} obtained from our best potential, but the actual frequencies are not known well enough.

Another possibility is that we are observing vibrational autodetachment of highly excited rovibrational states with energies above the electron detachment threshold. The $v_2 = 4$ state, for instance, lies very close to the electron continuum. In order for the electron of a vibrationally excited anion to detach, the mechanism must involve a breakdown of the Born–Oppenheimer approximation. Very little is known about such vibrational autodetachment rates. Our fast component decays at a rate that is four to seven orders of magnitude slower than the NH^- rotational autodetachment rates observed by Neumark, Lykke, Andersen, and Lineberger,³⁰ and three orders of magnitude slower than the SF_6^- autodetachment rates.³¹ These experiments are sensitive to fast processes, and cannot measure slower rates, whereas the experiment reported here can only measure long decays.

Thus, long-lived autodetaching states may have been present but unobserved in the earlier experiments. However, rovibrational states of CH_2^- that are metastable to detachment may not be long lived. There is a crossing of the CH_2 anion and neutral potential energy curves possibly near $v_2 = 0$ of the neutral.⁷ The propensity rules of Simons indicate that such a crossing would result in rapid electron detachment from any anion states above the detachment threshold.³²

None of these possibilities is entirely satisfactory. Thus, the identity of a component with $\tau = 14$ ms remains unclear, and the discrepancy between the *ab initio* results and the experimental data is unresolved.

V. CONCLUDING REMARKS

The best theoretical estimates of the radiative decay lifetimes of the bending mode of CH_2^- are 431, 207, 118, and 68 ms for the $v_2 = 1, 2, 3$, and 4 states, respectively. From a fit to a three exponential model the measured values are 500^{+50}_{-230} , 70^{+50}_{-40} , and 14^{+7}_{-7} ms. The first value is consistent with the $v_2 = 1$ theoretical lifetime but the remaining two are significantly shorter than predicted by theory. If the data are fit to a sum of four exponentials (assuming a geometric progression of lifetimes), we again find that the two shortest lifetimes are less than the theoretical values. Furthermore, a model using the four theoretically determined lifetimes fails to fit the data at times less than 20 ms. The theoretical results are consistent with the experimentally observed decay curve only if we postulate contributions to the photodetachment signal from an additional state of CH_2^- with a 15 ms lifetime, that is not a bending vibrational state (at least for the lowest rotational state of a vibrational state). However, alternative explanations for this fast decay, such as due to stretching vibrational states or highly excited rovibrational states, are not entirely consistent with our observations and calculations either. Thus, the identity of the $\tau = 14$ ms component remains in doubt.

Experimental and theoretical studies of radiative decay lifetimes of vibrationally excited polyatomic molecules are very difficult, although many of the difficulties in this study are no doubt due to the anionic nature of CH_2^- . Consequently, in order to reach definitive assignments of the radiative decay lifetimes of CH_2^- , more exact theoretical methods will probably be needed and experimentally better signal-to-noise over a longer time range is required. There are two main areas in which the *ab initio* determinations could possibly be improved. The first is the method used for determining the electronic wave function or dipole moment surface. Ideally, one would like a large basis set (with *f* functions on C and *d* functions on H) coupled with a large MCSCF-CI. Secondly, coupling of all the vibrational motions would be preferable although it is not clear how large an effect this will produce. It is probably true, though, that the radiative decay lifetimes of the upper levels would be affected most. Finally, we would suggest that the best approach for definitive assignments of radiative decay lifetimes of polyatomic systems

would seem to be the coupling of theory and experiment, because the experimental results alone do not always allow unique assignments to be made.

ACKNOWLEDGMENTS

The authors thank Dr. P. R. Bunker for a copy of his SRB program and helpful correspondence. We also thank Professor W. C. Lineberger and Dr. D. G. Leopold for helpful discussions. This research was supported by the Director, Office of Energy Research, Office of Basic Energy Sciences, Chemical Sciences Division of the U. S. Department of Energy under Contract No. DE-AC03-76SF00098.

¹M. Okumura, L. I.-C. Yeh, D. Normand, J. J. H. van den Biesen, S. W. Bustamente, and Y. T. Lee, *Tetrahedron* **41**, 1423 (1985).

²R. R. Corderman and W. C. Lineberger, *Annu. Rev. Phys. Chem.* **30**, 347 (1979).

³B. K. Janousek and J. I. Brauman, *Gas Phase Ion Chemistry*, edited by M. T. Bowers (Academic, New York, 1979), Vol. 2, p. 53.

⁴P. C. Engelking, R. R. Corderman, J. J. Wendoloski, G. B. Ellison, S. V. O'Neil, and W. C. Lineberger, *J. Chem. Phys.* **74**, 5460 (1981).

⁵A. R. W. McKellar, P. R. Bunker, T. J. Sears, K. M. Evenson, R. J. Saykally, and S. R. Langhoff, *J. Chem. Phys.* **79**, 5251 (1983).

⁶D. G. Leopold, K. K. Murray, A. E. Stevens Miller, and W. C. Lineberger, *J. Chem. Phys.* **83**, 4849 (1985).

⁷(a) S.-K. Shih, S. D. Peyerimhoff, R. J. Buenker, and M. Perić, *Chem. Phys. Lett.* **55**, 206 (1978); (b) L. B. Harding and W. A. Goddard III, *Chem. Phys. Lett.* **55**, 217 (1978).

⁸P. R. Bunker and S. R. Langhoff, *J. Mol. Spectrosc.* **102**, 204 (1983).

⁹T. J. Lee and H. F. Schaefer, *J. Chem. Phys.* **83**, 1784 (1985).

¹⁰T. J. Lee, J. E. Rice, and H. F. Schaefer (to be published).

¹¹H.-J. Werner, P. Rosmus, and E.-A. Reinsch, *J. Chem. Phys.* **79**, 905 (1983).

¹²P. Rosmus and H.-J. Werner, *J. Chem. Phys.* **80**, 5085 (1984).

¹³U. Mänz, A. Zilch, P. Rosmus, and H.-J. Werner, *J. Chem. Phys.* **84**, 5037 (1986).

¹⁴P. Botschwina, *J. Mol. Spectrosc.* **117**, 173 (1986).

¹⁵P. Botschwina, *Chem. Phys. Lett.* **114**, 58 (1985).

¹⁶P. Botschwina, *Habilitationsschrift*, University of Kaiserslautern, 1984.

¹⁷T. J. Lee, R. B. Remington, Y. Yamaguchi, and H. F. Schaefer, *J. Chem. Phys.* (to be published).

¹⁸S. M. Adler-Golden, S. R. Langhoff, C. W. Bauschlicher, and G. D. Carney, *J. Chem. Phys.* **83**, 255 (1985).

¹⁹P. R. Bunker and B. M. Landsberg, *J. Mol. Spectrosc.* **67**, 374 (1977).

²⁰T. J. Sears and P. R. Bunker, *J. Chem. Phys.* **79**, 5265 (1983). This SRB potential is derived from Ref. 4.

²¹P. R. Bunker and T. J. Sears, *J. Chem. Phys.* **83**, 4866 (1985). This SRB potential is derived from Ref. 6.

²²S. W. Bustamente, M. Okumura, D. Gerlich, H. S. Kwok, L. R. Carlson, and Y. T. Lee, *J. Chem. Phys.* **86**, 508 (1987).

²³M. Okumura, L. I. Yeh, D. Normand, and Y. T. Lee, *J. Chem. Phys.* **85**, 1971 (1986).

²⁴F. B. van Duijneveldt, IBM Res. Dept. RJ945 (1971).

²⁵P. Saxe, D. J. Fox, H. F. Schaefer, and N. C. Handy, *J. Chem. Phys.* **77**, 5584 (1982).

²⁶Y. Osamura, Y. Yamaguchi, and H. F. Schaefer, *J. Chem. Phys.* **77**, 383 (1982).

²⁷J. E. Rice, R. D. Amos, N. C. Handy, T. J. Lee, and H. F. Schaefer, *J. Chem. Phys.* **85**, 963 (1986).

²⁸G. H. F. Diercksen, B. O. Roos, and A. J. Sadlej, *Chem. Phys.* **59**, 29 (1981).

²⁹K. Raghavachari and J. A. Pople, *Int. J. Quantum Chem.* **20**, 1067 (1981).

³⁰D. N. Neumark, K. R. Lykke, T. Andersen, and W. C. Lineberger, *J. Chem. Phys.* **83**, 4364 (1985).

³¹J. E. Delmore and A. D. Appelhans, *J. Chem. Phys.* **84**, 6238 (1986).

³²J. Simons, *J. Am. Chem. Soc.* **103**, 3971 (1981).